IUCrData

ISSN 2414-3146

4-Bromopyridinium trichloridostannate(II)

Felix Henkel and Hans Reuter*

Chemistry, Osnabrück University, Barabarstr. 7, 49069 Osnabrück, Germany. *Correspondence e-mail: hreuter@uos.de

Received 13 August 2026
Accepted 24 August 2026

Keywords: crystal structure; trichloridostannate(II)-ion; 4-bromopyridinium; tetrel bonds; π–π interaction.

CCDC reference: 2582901

Structural data: full structural data are available from iucrdata.iucr.org

Single crystals of the title salt, $(C_5H_5BrN)[SnCl_3]$ or [4-BrPyH][$SnCl_3$], were prepared from aqueous solutions of 4-bromopyridinium hydrochloride, [4-BrPyH]Cl, and tin dichloride, $SnCl_2$. The cation has bond lengths and angles similar to those found in its other salts. In its first coordination sphere, the anion has a trigonal–pyramidal, *tpy*, structure with the Sn^{II} atom at the apex and the three chlorine atoms at the base. The tin–chlorine bond lengths are all greater than 2.5 Å and the bond angles are all less than 92°, which indicates the presence of *tetrel* bonds. These occur along the twofold screw-axis in the *b*-axis direction and extend the coordination sphere of the tin atom to a highly distorted, 3_3-aaa octahedron. In the crystal, the cations are stacked parallel to one another at varying distances along the *a*-axis direction, with weak π–π interactions occurring on both sides. Additional N—H···Cl hydrogen bonds are bifurcated and weak.

3D view

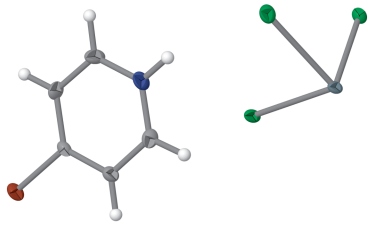

Chemical scheme

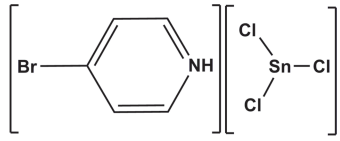

Structure description

The 4-bromopyrinium ion, $[4\text{-BrPyH}]^+$, is not only a cation frequently used in connection with transition-metal anions such as $[CuCl_4]^{2-}$ (Willett *et al.*, 2003), $[RuCl_6]^{2-}$ (Guthrie *et al.*, 2026), $[FeCl_4]^-$ (Zordan *et al.*, 2005) and $[CoHal_4]^-$ (Minguez Espallargas *et al.*, 2006), but also when it comes to crystallizing anions of low-valent *p*-block elements. Typical examples in this case are anions of trivalent antimony, such as $[Sb^{III}{}_2Hal_9]^{3-}$ (Nicolas *et al.*, 2022), trivalent bismuth, such as $[Bi^{III}{}_2Hal_{10}]^{4-}$ (Adonin *et al.*, 2018) or tetravalent tellurium, such as $[Te^{IV}I_6]^{2-}$ (Walusiak *et al.*, 2023). In this series of compounds, the title compound 4-bromopyridinium trichloridostannate(II), [^{4}BrpyH]-[$Sn^{II}Cl_3$], is the first to contain an anion of divalent tin.

The asymmetric unit (Fig. 1 and Table 1) comprises one formula unit of each ion with all atoms in general positions. The cation exhibits the well-known structural features evident from the preceding publications: (i) the backbone of the pyridinium ion is nearly planar [Δ = ±0.011 (5) Å], (ii) the bromine atom lies slightly outside [0.0921 (5) Å] this plane, (iii) the bond angle at the nitrogen atom is significantly widened [122.7 (4)°], (iv)

Table 1
Selected geometric parameters (Å, °).

Sn1—Cl3	2.5475 (12)	Sn1—Cl1	2.5745 (11)
Sn1—Cl2	2.5711 (12)		
Cl3—Sn1—Cl2	90.73 (4)	Cl2—Sn1—Cl1	88.30 (4)
Cl3—Sn1—Cl1	88.32 (4)		

the bond angles at the carbon atoms in the *meta* position relative to the nitrogen atom are significantly narrowed [117.8 (5)/118.5 (4)°], (v) within the ring, the N—C bond lengths [1.330 (7)/1.340 (6) Å] are shorter than the C—C bonds [mean value: 1.383 (6) Å] and (vi) a Br—C distance of 1.873 (5) Å.

With respect to the first coordination sphere, in which the Sn^{II} atom (Fig. 1) achieves an electron octet, the $[SnCl_3]^-$ ion exhibits a trigonal–pyramidal, *tpy*, structure, with the tin atom at the apex and the three chlorine atoms in the basal plane. Given bond angles of around 90°, it can be assumed that the three empty, orthogonal 5*p* orbitals of the tin(II) atom are involved in the bonds.

Based on their structural parameters, the trichloridostannate(II) ions ions can be divided into two groups: in the first group, the tin–chlorine bond lengths are with a few exceptions shorter than 2.50 Å and the bond angles are all greater than 92°. This group includes, for example, the trichloridostannate(II) ions found in the compounds $[Ph_4P][SnCl_3]$ (Müller *et al.*, 1982), $[Sn^{II}Cl(18\text{-crown-6})][SnCl_3]$ (Drew & Nicholson, 1986) and $[Hf^{IV}(O^tBu)_3(thf)_3][SnCl_3]$ (Njua *et al.*, 2010). In the second group, one, two or all three tin–chlorine bonds are longer than 2.50 Å and one or more bond angles are less than 90°. Typical examples are: [MPyrH][$SnCl_3$] (MPyrH = 1-methylpyrrolidin-1-ium; Liu *et al.*, 2019), [Li(12-crown-4)(thf)][SnCl3] (Izod *et al.*, 2012) and [$^tBuNH_3$][$SnCl_3$] (Veith *et al.*, 1988). In the first group, these are "naked" ions without strong intermolecular interactions involving the Sn^{II} atom with other building units; in the second

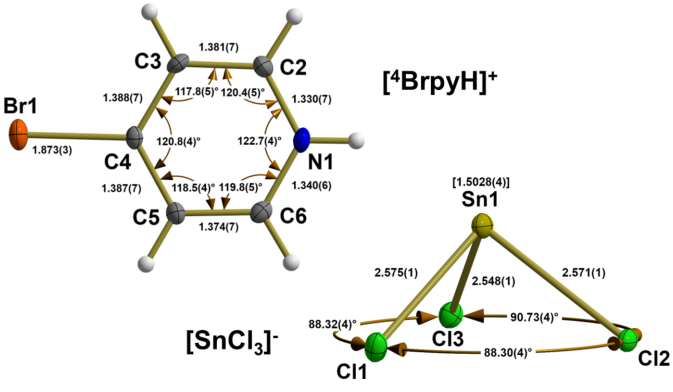

Figure 1
The [4-BrPyH]$^+$ and $[SnCl_3]^-$ ion of the asymmetric unit with atom numbering, bond lengths (Å), bond angles (°) and distance of the tin atom from the basal plane in square brackets. With the exception of the hydrogen atoms, which are shown as spheres of arbitrary radius, all other atoms are drawn as anisotropic displacement ellipsoids at the 50% probability level.

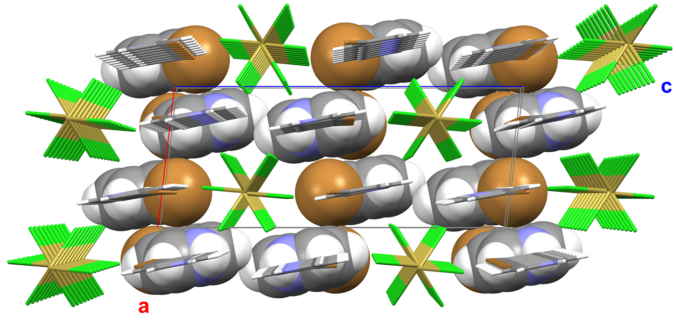

Figure 2
Perspective view into the crystal of [4-BrPyH][$SnCl_3$] looking down the *b* axis. All components are drawn as stick models with the cations in the background additionally represented as space-filling models. Colour code and van der Waals radii used: Sn = bronze, Cl = green, C = dark grey, 1.70 Å, H = white, 1.20 Å, N = light- blue, 1.55 Å, Br = brown, 1.85 Å.

group, they are ions in which the Sn^{II} atoms form additional so-called *tetrel bonds* (Bauzá *et al.*, 2019; Brammer *et al.*, 2023), characterized by the fact that they occur in a *trans* position to existing strong 2*c*–2*e* bonds. In the broadest sense, *tetrel bonds* can be regarded as extensive 3*c*–4*e* bonds based on an almost linear alignment of the *p*-orbitals of the three atoms involved in the *X*—Sn···Y arrangement (Reuter, 2025).

Based on the structural parameters observed in present case, the $[SnCl_3]^-$ ion must, unambiguously, be classified in the second group. A look inside the crystal (Fig. 2) reveals that the anions are arranged in rows along the *b* axis with alternating orientations caused by a twofold crystallographic screw axis in the *b*-axis direction (Fig. 3), while the cations are stacked in a

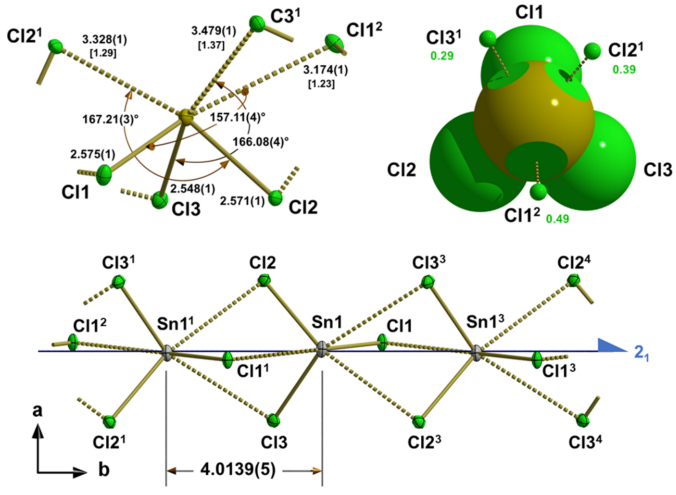

Figure 3
Different representation of the tetrel bonds linking the $[SnCl_3]^-$ ions. (above, left) ball-and-stick model of the tin environment with geometric parameters (Å, °) and asymmetry parameters *Q* (values in square brackets) characterizing the tetrel bonds, (above, right) space-filling model visualizing the inter-penetration of the van der Waals radii of tin and chlorine as result of the tetrel bond formation and interpenetration indices *p* (green values), (below) side-view on the twofold screw axis causing the tetrel-bond formation with the distance (Å) between two neighbouring tin atoms. Symmetry codes used to generate equivalent atoms: (1) $\frac{3}{2}-x,\frac{1}{2}+y,\frac{1}{2}-z$; (2) $\frac{3}{2}-x,-\frac{1}{2}+y,\frac{1}{2}-z$.

Table 2
Geometric details (Å), asymmetry parameters Q, bond valences BV and interpenetration indices p characterizing the tetrel bonds.

X/Y	d(Sn—X)	d(Sn···Y)	⟨(X—Sn···Y)	Q	BV(Sn···Y)	BV(Sn—X)	p(Sn···Y)
Cl1/Cl1^{2}	2.575 (1)	3.174 (3)	167.21 (3)°	1.23	0.05	0.60	0.49
Cl2/Cl2^{1}	2.571 (1)	3.328 (3)	166.08 (4)°	1.29	0.07	0.57	0.39
Cl3/Cl3^{1}	2.548 (1)	3.479 (3)	157.11 (4)°	1.37	0.11	0.56	0.29
Sum					0.23	1.73	

Symmetry codes: (1) $\frac{3}{2}-x,\frac{1}{2}-y,\frac{1}{2}-z$; (2) $\frac{3}{2}-x,-\frac{1}{2}-y,\frac{1}{2}-z$.

Table 3
Hydrogen-bond geometry (Å, °).

D—H···A	D—H	H···A	D···A	D—H···A
N1—H1···Cl2^{i}	0.88	2.77	3.357 (4)	125
N1—H1···Cl3	0.88	2.48	3.255 (4)	147

staggered arrangement along the *a* axis. In the case of the anions, the interactions result in three *tetrel bonds* (Fig. 3*a*, Table 2). With an asymmetry quotient $Q = d(\mathrm{Sn}\cdots\mathrm{Cl})/d(\mathrm{Sn}—\mathrm{Cl}) = 1.365$ (Cl3), 1.294 (Cl2) and 1.233 (Cl1), these 3*c*–4*e* bonds are highly asymmetric, causing the *tpy*, 3_0 configuration (Schröder *et al.*, 2024), of the first coordination sphere being extended to a highly distorted octahedral, 3_3-aaa configuration. Similarly, the inter-penetration indices ρ (Echeverriá & Alvarez, 2023) using the van der Waals radii [r_{vdW}(Cl) = 1.75 Å and r_{vdW}(Sn) = 2.17 Å; Cordero *et al.*, 2008] and the covalent radii [r_{cov}(Cl) = 1.02 Å and r_{cov}(Sn) = 1.39 Å; Mantina *et al.*, 2009] support this concept. Furthermore, the calculation of bond valences, BS, according to Brese & O'Keeffe (1991) [R_{ij} = 2.36, b = 0.37] shows that the intermolecular Sn···Cl distances contribute only slightly [0.23] to the calculated bond valence sum [$\mathrm{BVS_{cal}}$ = 1.96] of the divalent tin atom.

The 4-bromopyridinium ions are stacked exactly parallel to one another, as they are flanked on both sides by crystallographic centres of symmetry at (0,0,0; Wyckhoff letter: *a*) and (1/2,0,0; Wyckhoff letter: *d*). The overlap of the pyridinium units, and thus the π–π interaction, is limited to the nitrogen atoms and two neighbouring carbon atoms (Fig. 4*a*). In this context, the extent of the overlap correlates with the distances between the least-squares planes defined by the ring atoms of neighbouring molecules (Fig. 4*b*): in the case of the centres of symmetry at *a*, the distance is significantly shorter (3.08 Å) and the overlap smaller than in the case of the centers of symmetry at *d* (3.84 Å) where the overlap is larger.

In addition to their contribution to the tetrel bonds, the chlorine atoms, Cl2 and Cl3, are involved into hydrogen bonds with the hydrogen atom attached to the nitrogen atom of the 4-bromopyridinium ion (Table 3). The donor–acceptor distances are quite long, as the hydrogen bond is bifurcated.

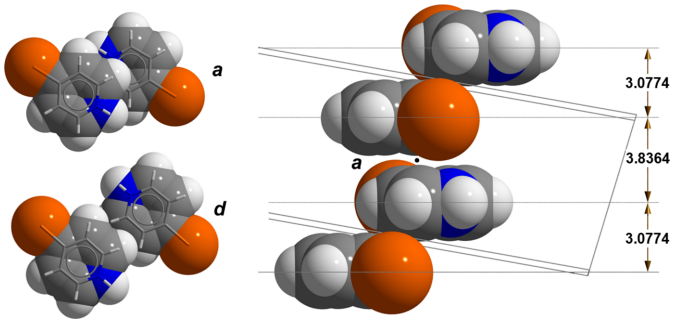

Figure 4
Different representations of the cation stacking. (left) Space-filling model with stick model overlayed viewed perpendicular to the least-squares planes showing the extend of the overlap as resulting from the different centres of symmetry in Wyckoff positions *a*, and *d*. (right) Space-filling model of the stacking sequence in side-view with distances [Å] between the least-squares planes; from the two different centres of symmetry (black dots) responsible for the stacking sequence only the one at (1/2,1/2,1/2), Wyckoff position *a* is visible.

Synthesis and crystallization

Stannous chloride (0.146 g (0.77 mmol); Sigma-Aldrich) was dissolved in approximately 10 ml of water together with

Table 4
Experimental details.

Crystal data	
Chemical formula	$(C_5H_5BrN)[SnCl_3]$
M_r	384.05
Crystal system, space group	Monoclinic, $P2_1/n$
Temperature (K)	100
a, b, c (Å)	7.2468 (2), 8.0253 (3), 17.7393 (6)
β (°)	96.834 (2)
V (Å^3)	1024.35 (6)
Z	4
Radiation type	Mo $K\alpha$
μ (mm^{-1})	7.12
Crystal size (mm)	0.15 × 0.12 × 0.04
Data collection	
Diffractometer	Bruker APEXII CCD
Absorption correction	Multi-scan (*SADABS*; Krause *et al.*, 2015)
T_{min}, T_{max}	0.415, 0.774
No. of measured, independent and observed [$I > 2\sigma(I)$] reflections	97897, 2562, 2231
R_{int}	0.079
(sin $\theta/\lambda)_{max}$ (Å^{-1})	0.668
Refinement	
$R[F^2 > 2\sigma(F^2)]$, $wR(F^2)$, S	0.030, 0.073, 1.28
No. of reflections	2562
No. of parameters	101
H-atom treatment	Only H-atom displacement parameters refined
$\Delta\rho_{max}$, $\Delta\rho_{min}$ (e Å^{-3})	1.40, −0.91

Computer programs: *APEX2* and *SAINT* (Bruker, 2009), *SHELXS97* (Sheldrick, 2008), *SHELXL2014/7* (Sheldrick, 2015), *DIAMOND* (Brandenburg, 2006) and *Mercury* (Macrae *et al.*, 2020) and *publCIF* (Westrip, 2010).

0.150 g (0.77 mmol) of 4-bromopyridine hydrochloride. Upon slow evaporation of the aqueous solutions at room temperature, the title compound crystallized out in the form of colourless blocks. Yield: 0.256 g (86% of the theoretical yield).

Refinement

Crystal data, data collection and structure refinement details are summarized in Table 4. The maximum and minimum residual electron density peaks of 1.40 and −0.91 e Å^{-3}, respectively, were located 1.99 and 1.97 Å from the H6 and Sn1 atoms, respectively.

Acknowledgements

We thank the Deutsche Forschungsgemeinschaft and the Government of Lower-Saxony for funding the diffractometer and acknowledge support by Deutsche Forschungsgemeinschaft (DFG) and Open Access Publishing Fund of Osnabrück University.

References

Adonin, S. A., Gorokh, I. D., Novikov, A. S., Samsonenko, D. G., Yushina, I. V., Sokolov, M. N. & Fedin, V. P. (2018). *CrystEngComm* **20**, 7766–7772.
Bauzá, A., Seth, S. K. & Frontera, A. (2019). *Coord. Chem. Rev.* **384**, 107–125.
Brammer, L., Peuronen, A. & Roseveare, T. M. (2023). *Acta Cryst.* C**79**, 204–216.
Brandenburg, K. (2006). *DIAMOND*. Crystal Impact GbR, Bonn, Germany.
Brese, N. E. & O'Keeffe, M. (1991). *Acta Cryst.* B**47**, 192–197.
Bruker (2009). *APEX2* and *SAINT* . Bruker AXS Inc., Madison, Wisconsin, USA.
Cordero, B., Gómez, V., Platero-Prats, A. E., Revés, M., Echeverría, J., Cremades, E., Barragán, F. & Alvarez, S. (2008). *Dalton Trans.* pp. 2832.
Drew, M. G. B. & Nicholson, D. G. (1986). *J. Chem. Soc. Dalton Trans.* **15**, 1543–1549.
Echeverría, J. & Alvarez, S. (2023). *Chem. Sci.* **14**, 11647–11688.
Guthrie, H. D., Stone, S. R. P., Schofield, M. H. & Cahill, C. L. (2026). *Cryst. Growth Des.* **26**, 2325–2338.
Izod, K., Clark, E. R., Clegg, W. & Harrington, R. W. (2012). *J. Organomet. Chem.* **31**, 246–255.
Krause, L., Herbst-Irmer, R., Sheldrick, G. M. & Stalke, D. (2015). *J. Appl. Cryst.* **48**, 3–10.
Liu, X., Ji, C., Wu, Z., Li, L., Han, S., Wang, Y., Sun, Z. & Luo, J. (2019). *Chem. Eur. J.* **25**, 2610–2615.
Macrae, C. F., Sovago, I., Cottrell, S. J., Galek, P. T. A., McCabe, P., Pidcock, E., Platings, M., Shields, G. P., Stevens, J. S., Towler, M. & Wood, P. A. (2020). *J. Appl. Cryst.* **53**, 226–235.
Mantina, M., Chamberlin, A. C., Valero, R., Cramer, C. J. & Truhlar, D. G. (2009). *J. Phys. Chem. A* **113**, 5806–5812.
Mínguez Espallargas, G., Brammer, L. & Sherwood, P. (2006). *Angew. Chem. Int. Ed.* **45**, 435–440.
Müller, U., Mronga, N., Schuhmacher, C. & Dehnike, K. (1982). *Z. Naturforsch.* **B37**, 1122–1127.
Nicholas, A. D., Garman, L. C., Albano, N. & Cahill, C. L. (2022). *Phys. Chem. Chem. Phys.* **24**, 15305–15320.
Njua, E. Y., Steiner, A. & Stahl, L. (2010). *Inorg. Chem.* **49**, 2163–2172.
Reuter, H. (2025). *Molecules* **30**, 2700.
Schröder, S., Röwekamp-Krugley, N., Imwalle, M. & Reuter, H. (2024). *Z. Anorg. Allg. Chem.* **650**, e202400091.
Sheldrick, G. M. (2008). *Acta Cryst.* A**64**, 112–122.
Sheldrick, G. M. (2015). *Acta Cryst.* C**71**, 3–8.
Veith, M., Jarczyk, M. & Huch, M. (1988). *Chem. Ber.* **121**, 347–355.
Walusiak, B. W., Raghavan, A. & Cahill, C. L. (2023). *RSC Adv.* **13**, 13477–13492.
Westrip, S. P. (2010). *J. Appl. Cryst.* **43**, 920–925.
Willett, R. D., Awwadi, F., Butcher, R., Haddad, S. & Twamley, B. (2003). *Cryst. Growth Des.* **3**, 301–311.
Zordan, F., Purver, S. L., Adams, H. & Brammer, L. (2005). *CrystEngComm* **7**, 350–354.

full crystallographic data

IUCrData (2026). **11**, x260877 [https://doi.org/10.1107/S2414314626008771]

4-Bromopyridinium trichloridostannate(II)

Felix Henkel and Hans Reuter

4-Bromopyridinium trichloridostannate(II)

Crystal data

$(C_5H_5BrN)[SnCl_3]$
M_r = 384.05
Monoclinic, $P2_1/n$
a = 7.2468 (2) Å
b = 8.0253 (3) Å
c = 17.7393 (6) Å
β = 96.834 (2)°
V = 1024.35 (6) Å^3
Z = 4
$F(000)$ = 712
D_x = 2.490 Mg m^{-3}
Mo $K\alpha$ radiation, λ = 0.71073 Å
Cell parameters from 9904 reflections
θ = 2.3–27.5°
μ = 7.12 mm^{-1}
T = 100 K
Bloc, colourless
0.15 × 0.12 × 0.04 mm

Data collection

Bruker APEXII CCD diffractometer
φ and ω scans
Absorption correction: multi-scan (SADABS; Krause *et al.*, 2015)
T_{min} = 0.415, T_{max} = 0.774
97897 measured reflections
2562 independent reflections
2231 reflections with $I > 2\sigma(I)$
R_{int} = 0.079
θ_{max} = 28.3°, θ_{min} = 2.8°
h = −9→9
k = −10→10
l = −23→23

Refinement

Refinement on F^2
Least-squares matrix: full
$R[F^2 > 2\sigma(F^2)]$ = 0.030
$wR(F^2)$ = 0.073
S = 1.28
2562 reflections
101 parameters
0 restraints
Primary atom site location: structure-invariant direct methods
Hydrogen site location: inferred from neighbouring sites
Only H-atom displacement parameters refined
$w = 1/[\sigma^2(F_o^2) + (0.0158P)^2 + 6.4943P]$ where $P = (F_o^2 + 2F_c^2)/3$
$(\Delta/\sigma)_{max}$ = 0.001
$\Delta\rho_{max}$ = 1.40 e Å^{-3}
$\Delta\rho_{min}$ = −0.91 e Å^{-3}

Special details

Geometry. All esds (except the esd in the dihedral angle between two l.s. planes) are estimated using the full covariance matrix. The cell esds are taken into account individually in the estimation of esds in distances, angles and torsion angles; correlations between esds in cell parameters are only used when they are defined by crystal symmetry. An approximate (isotropic) treatment of cell esds is used for estimating esds involving l.s. planes.

Refinement. The H atoms were refined in idealized geometries and allowed to ride on the parent carbon [d(C—H) = 0.95 Å] and nitrogen atoms [d(N—H) = 0.88 Å] with one common isotropic temperature factor.

Fractional atomic coordinates and isotropic or equivalent isotropic displacement parameters (Å²)

	x	*y*	*z*	U_{iso}*/U_{eq}
Sn1	0.75694 (5)	0.43421 (4)	0.24976 (2)	0.01293 (9)
Cl1	0.78133 (17)	0.63009 (14)	0.36546 (6)	0.0161 (2)
Cl2	1.00513 (16)	0.24850 (15)	0.32359 (6)	0.0159 (2)
Cl3	0.50030 (16)	0.27775 (15)	0.30640 (7)	0.0180 (2)
Br1	0.24791 (7)	1.05162 (6)	0.52167 (3)	0.01847 (12)
N1	0.2791 (6)	0.5686 (5)	0.3868 (2)	0.0182 (8)
H1	0.2893	0.4752	0.3616	0.034 (8)*
C4	0.2545 (6)	0.8551 (6)	0.4651 (3)	0.0137 (9)
C5	0.2871 (7)	0.8616 (6)	0.3896 (3)	0.0174 (10)
H5	0.2998	0.9652	0.3648	0.034 (8)*
C6	0.3003 (7)	0.7125 (6)	0.3517 (3)	0.0177 (10)
H6	0.3248	0.7128	0.3003	0.034 (8)*
C2	0.2428 (8)	0.5598 (7)	0.4590 (3)	0.0220 (11)
H2	0.2260	0.4545	0.4817	0.034 (8)*
C3	0.2299 (8)	0.7035 (6)	0.5002 (3)	0.0204 (11)
H3	0.2048	0.6993	0.5515	0.034 (8)*

Atomic displacement parameters (Å²)

	U^{11}	U^{22}	U^{33}	U^{12}	U^{13}	U^{23}
Sn1	0.01820 (16)	0.00819 (14)	0.01255 (14)	0.00055 (13)	0.00242 (11)	−0.00069 (12)
Cl1	0.0255 (6)	0.0100 (5)	0.0128 (5)	0.0000 (4)	0.0024 (4)	−0.0014 (4)
Cl2	0.0160 (5)	0.0147 (5)	0.0171 (5)	0.0021 (4)	0.0020 (4)	−0.0018 (4)
Cl3	0.0166 (5)	0.0159 (5)	0.0223 (6)	−0.0020 (4)	0.0052 (4)	−0.0052 (4)
Br1	0.0200 (2)	0.0136 (2)	0.0216 (2)	−0.00019 (19)	0.00136 (18)	−0.00675 (19)
N1	0.023 (2)	0.015 (2)	0.0169 (19)	0.0013 (18)	0.0026 (16)	−0.0060 (17)
C4	0.013 (2)	0.012 (2)	0.016 (2)	0.0024 (17)	0.0010 (17)	−0.0023 (18)
C5	0.022 (3)	0.013 (2)	0.017 (2)	0.0022 (19)	0.0036 (19)	−0.0010 (19)
C6	0.019 (2)	0.021 (3)	0.014 (2)	−0.0008 (19)	0.0030 (18)	−0.0022 (19)
C2	0.037 (3)	0.012 (2)	0.018 (2)	−0.002 (2)	0.005 (2)	0.000 (2)
C3	0.031 (3)	0.021 (3)	0.011 (2)	0.001 (2)	0.008 (2)	−0.0009 (19)

Geometric parameters (Å, º)

Sn1—Cl3	2.5475 (12)	C4—C5	1.388 (7)
Sn1—Cl2	2.5711 (12)	C5—C6	1.381 (7)
Sn1—Cl1	2.5745 (11)	C5—H5	0.9500
Br1—C4	1.873 (5)	C6—H6	0.9500
N1—C6	1.330 (7)	C2—C3	1.374 (7)
N1—C2	1.340 (6)	C2—H2	0.9500
N1—H1	0.8800	C3—H3	0.9500
C4—C3	1.387 (7)		
Cl3—Sn1—Cl2	90.73 (4)	C4—C5—H5	121.1
Cl3—Sn1—Cl1	88.32 (4)	N1—C6—C5	120.4 (5)

Cl2—Sn1—Cl1	88.30 (4)	N1—C6—H6	119.8
C6—N1—C2	122.7 (4)	C5—C6—H6	119.8
C6—N1—H1	118.7	N1—C2—C3	119.8 (5)
C2—N1—H1	118.7	N1—C2—H2	120.1
C3—C4—C5	120.8 (4)	C3—C2—H2	120.1
C3—C4—Br1	119.0 (4)	C2—C3—C4	118.5 (4)
C5—C4—Br1	120.2 (4)	C2—C3—H3	120.8
C6—C5—C4	117.8 (5)	C4—C3—H3	120.8
C6—C5—H5	121.1		

Hydrogen-bond geometry (Å, º)

D—H···*A*	*D*—H	H···*A*	*D*···*A*	*D*—H···*A*
N1—H1···Cl2^{i}	0.88	2.77	3.357 (4)	125
N1—H1···Cl3	0.88	2.48	3.255 (4)	147

Symmetry code: (i) $x-1, y, z$.